Scattering times of the two-dimensional electron gas on silicon (111) with a density dependent effective mass

2007 J. Phys.: Condens. Matter 19 506214

(http://iopscience.iop.org/0953-8984/19/50/506214)

IOP PUBLISHING JOURNAL OF PHYSICS: CONDENSED MATTER

J. Phys.: Condens. Matter **19** (2007) 506214 (12pp) doi:10.1088/0953-8984/19/50/506214

Scattering times of the two-dimensional electron gas on silicon (111) with a density dependent effective mass

A Gold

Centre d'Elaboration de Materiaux et d'Etudes Structurales (CEMES-CNRS),
29 Rue Jeanne Marvig, 31055 Toulouse, France

Received 28 August 2007, in final form 18 October 2007
Published 21 November 2007
Online at stacks.iop.org/JPhysCM/19/506214

Abstract

For temperature zero we calculate the transport scattering time and the single-particle relaxation time of the two-dimensional electron gas on the surface of silicon (111). For the transport scattering time we take into account the existence of a metal–insulator transition while the single-particle relaxation time is not sensitive to a metal–insulator transition. Agreement with experimental results on the mobility and the transport scattering time is obtained by using a density dependent effective mass, taken from experiment. We discuss the astonishing behavior of the single-particle relaxation time in our calculation which is, however, in agreement with experiment. The mass divergence found in experiment is discussed within the frame of Bloch's quantum phase transition from a paramagnetic phase to an ordered phase at low electron density. We argue that the ordered phase represents a valley-polarized ground state (or an antiferromagnetic ground state).

1. Introduction

For decades the transport properties of the two-dimensional electron gas (2DEG) have been a very exciting research area [1]. In recent years some interesting experiments have been made in the low-electron-density range of the 2DEG, where interaction effects are very strong and where new ground states can be expected. The essential parameter to measure interaction effects is the Wigner–Seitz parameter r_s given by the electron density N and the effective Bohr radius a_B^* and expressed as $r_s = 1/\sqrt{\pi N a_B^{*2}}$. This parameter gives, for the single-valley case $g_v = 1$, the ratio of the mean Coulomb energy E_C to the Fermi energy E_F: $r_s = E_C/E_F$. It follows that for small density this parameter becomes large and, from a theoretical point of view, perturbation theory becomes questionable.

The 2DEG in silicon-MOSFET (metal–oxide–semiconductor field-effect transistor) structures on the (100) surface is an important testing ground due to the larger effective mass and the larger valley degeneracy $g_v = 2$ compared to the two-dimensional electron gas realized in GaAs where $g_v = 1$. Interaction effects and many-body effects increase in systems with increasing valley degeneracy [2]. However, silicon-MOSFET structures contain more disorder

than GaAs heterostructures. It is well known that in silicon-MOSFET structures with low peak-mobility $\mu_{\rm peak} < 5\times10^3$ cm^2 V^{-1} s^{-1} a metal–insulator transition (MIT) occurs at low electron density [1]. The mobility data can be explained by a transport theory including an MIT [3]. At the metal–insulator transition the mobility and, therefore, also the transport scattering time at zero temperature vanishes. In silicon (100) MOSFET structures with high peak-mobility $\mu_{\rm peak} \approx 3.5 \times 10^4$ cm^2 V^{-1} s^{-1} such an MIT also occurs, but at a very low electron density $N_{\rm MIT}^{\rm Si(100)} \approx 0.8 \times 10^{11}$ cm^{-2} [4]. Some years ago it was found that, besides the existence of an MIT in silicon (100), a strong mass enhancement also occurs, with a trend to diverge at a critical density $N_{\rm cm}$, which is near to the density of the MIT $N_{\rm cm}^{\rm Si(100)} \approx N_{\rm MIT}^{\rm Si(100)}$ [5]. This mass enhancement was first measured using a parallel magnetic field. The origin of this mass divergence is not known and was confirmed with other experimental techniques, for instance with the Shubnikov-de Haas (SdH) effect [6] and with measurements of the magnetic susceptibility [7]. For a review, see [8]. Some effort has been undertaken to observe this mass divergence in other systems, for instance in the 2DEG realized in AlAs quantum wells [9, 10] and in GaAs heterostructures [11, 12]. However, no mass divergence was found in these systems.

The valley degeneracy of the 2DEG on the surface of silicon (111) should be 6. Experimentally, however, one usually finds $g_{\rm v} = 2$ [1, 13]. In a theoretical analysis [14] on low temperature transport data of silicon (111) with a peak mobility of $\mu_{\rm peak} \approx 2.4 \times 10^3$ cm^2 V^{-1} s^{-1} it was argued that an MIT occurs. Very recently the mobility and the temperature dependence of SdH oscillations of the 2DEG on the surface of silicon (111) have been studied in detail [15]. These measurements clearly confirmed the existence of an MIT at $N_{\rm MIT}^{\rm Si(111)} \approx 3 \times 10^{11}$ cm^{-2}. In addition, a strong mass enhancement with the possibility of a diverging mass at $N_{\rm cm}^{\rm Si(111)} \approx N_{\rm MIT}^{\rm Si(111)}$ was found. It was argued [15] that the diverging mass is due to interaction effects, because the mass divergence of the 2DEG in silicon (100) and silicon (111) occurred at the same Wigner–Seitz parameter $r_{\rm s} \approx 9.5$. In fact, $N_{\rm cm}^{\rm Si(100)}/N_{\rm cm}^{\rm Si(111)} \approx 0.27$ corresponds to the squared mass ratio of silicon (100) with $m^* = 0.19m_{\rm e}$ and silicon (111) with $m^* = 0.36m_{\rm e}$, written as $(0.19/0.36)^2 = 0.28$, which represents the squared ratio of the effective Bohr radii.

The mass divergence in silicon (100) and (111) occurs always very near to an MIT. One may ask if the MIT is connected to the mass divergence. In the argument put forward in [15] disorder does not play any role. Independently of the question of whether disorder is important for the mass divergence, very interesting low temperature transport properties as a function of the electron density have been reported near $N_{\rm cm}^{\rm Si(111)} \approx N_{\rm MIT}^{\rm Si(111)}$ [15]. These data are discussed in the first part of the paper. From experimental results obtained for different 2DEGs [4–7, 9–12, 15] in the second part of the paper we describe a possible scenario leading to the novel mass divergence.

The paper is organized as follows. In section 2 we describe our model and the theory for the different scattering times. Numerical results for the transport scattering time and the single-particle relaxation time according to our theory and comparison with experiments on silicon (111) are presented in section 3. In section 4 we discuss the origin of the mass divergence within the concept of a quantum phase transition. We present our summary in section 5.

2. Model and theory

2.1. Model

Two scattering times determine transport experiments: the transport scattering time $\tau_{\rm t}$, accessible in transport measurements, and the single-particle relaxation time $\tau_{\rm s}$, accessible in

SdH measurements [1, 16, 17]. In the lowest order theory the two scattering times should be finite and behave similarly. However, at the MIT the transport scattering time τ_t vanishes in the limit of vanishing temperature. This corresponds to the definition of an MIT due to disorder: with a finite mobility (conductivity) in the metallic phase and a vanishing mobility (conductivity) in the insulating phase at zero temperature. In SdH measurements, used to measure the effective mass m^*, one also has access to the single-particle relaxation time. This scattering time is related to the Dingle temperature [1]. τ_s represents a measure of how disorder modifies the density of states in the presence of disorder in the limit of a vanishing magnetic field. If the density of states is finite at the MIT then τ_s is finite, too. This is because multiple scattering effects give only small modifications to τ_s, if compared to the contribution of multiple scattering effects to τ_t [17]. The ratio $\tau_t/\tau_s \to 0$ should, therefore, vanish at the MIT.

In the following we present the results of our calculation of the transport scattering time and the single-particle relaxation time. We compare them with recent experimental results found for the 2DEG on silicon (111) [15]. Experimentally only a mass enhancement of about 3 was measured. But the experiment strongly suggests such a divergent mass at a finite electron density N_{cm}. The lowest mobility measured in [15] at a temperature of 30 mK was smaller than 1% of the peak mobility, indicating a real MIT at the finite electron density N_{MIT}.

For the calculation of the transport scattering time and the single-particle relaxation time we used the lowest order theory, where $1/\tau_t^o$ and $1/\tau_s^o$ are proportional to the random potential $\langle|U(q)|^2\rangle$ created by the disorder. Screening effects are described within the random-phase approximation (RPA) [18]. Many-body effects beyond the RPA are treated by using the local-field correction $G(q)$ in the Hubbard approximation $G_H(q)$ [19]. Charged impurity scattering (CIS) and interface-roughness scattering (IRS) have been taken into account. They represent the two relevant scattering mechanisms: CIS is most important at low electron density and IRS is important at high electron density [1]. The finite width of the electron gas is described by form factors, which can be found in [1]. The depletion density is $N_D = 1 \times 10^{11}$ cm^{-2}.

2.2. Theory

The expression for the transport scattering time in the lowest order (o) of the random potential is given by [17]

$$\frac{\hbar}{\tau_t^o} = \frac{1}{2\pi\varepsilon_F}\int_0^{2k_F} dq\,\frac{\langle|U(q)|^2\rangle}{\varepsilon(q)^2}\frac{q^2}{(4k_F^2-q^2)^{1/2}}. \tag{1}$$

$\langle|U(q)|^2\rangle$ represents the random potential due to CIS and IRS. ε_F is the Fermi energy and k_F the Fermi wavenumber. We use the screening function

$$\varepsilon(q \leqslant 2k_F) = 1 + q_s[1 - G(q)]F_c(q)/q, \tag{2}$$

where $q_s = 2g_v/a_B^*$ is the screening wavenumber. a_B^* is the effective Bohr radius $a_B^* = a_B^0\varepsilon_L m_e/m^*$ which depends on the background dielectric constant ε_L and the effective mass m^*. $a_B^0 = 0.53$ Å is the Bohr radius in free space. $F_c(q)$ represents the form factor for the Coulomb interaction due to the finite width [1]. The single-particle relaxation time in the lowest order of the random potential is given by

$$\frac{\hbar}{\tau_s^o} = \frac{1}{2\pi\varepsilon_F}\int_0^{2k_F} dq\,\frac{\langle|U(q)|^2\rangle}{\varepsilon(q)^2}\frac{2k_F^2}{(4k_F^2-q^2)^{1/2}} \tag{3}$$

and this equation is valid for $\varepsilon_F\tau_s^o > \hbar$ [17].

Within an analysis for the mass dependence for $2k_F \ll q_s$ one finds $1/\tau_s^o \propto 1/\varepsilon_F q_s^2 \propto m^* a_B^{*2} \propto 1/m^*$. Therefore we conclude that $\tau_t^o \propto \tau_s^o \propto m^*$. A divergence of the effective mass m^* implies a divergence of both scattering times, calculated in lowest order of the disorder.

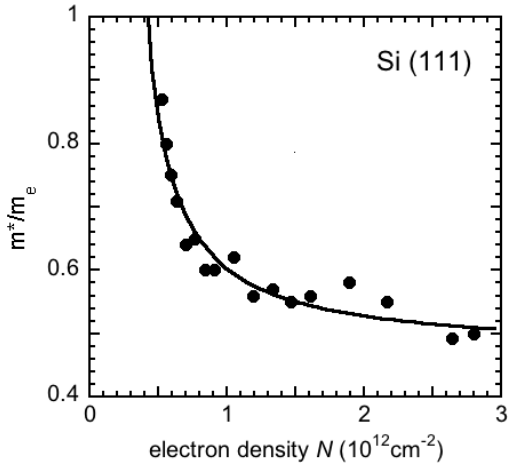

Figure 1. Effective mass m^* in units of the free electron mass m_e as a function of electron density N for silicon (111). The solid dots are experimental results according to [15]. The solid line represents a fit to the experiment according to $m^*/m_e = 0.46/(1 - N_{cm}/N)$ with $N_{cm} = 2.2 \times 10^{11}$ cm^{-2}.

When the effective mass is enhanced, a_B^* decreases and approaches zero when the effective mass diverges. This means that the screening properties are improved when mass enhancement occurs.

For the transport scattering time we take into account multiple scattering effects. They are very important near N_{MIT} and are the origin for the MIT [20]. Therefore a modified expression for the mobility was used: at the MIT the mobility goes to zero and the mobility for all densities is well described by the form $\mu(N > N_{MIT}) = \mu^o(N)(1 - N_{MIT}/N) \equiv e\tau/m^*$ and $\mu(N < N_{MIT}) = 0$ [21]. $\mu^o(N) = e\tau_t^o/m^*$ represents the mobility calculated in the lowest order of the random potential. Note that $\mu(N \gg N_{MIT}) \approx \mu^o(N)$ while near the MIT the mobility is expressed by $\mu(N \approx N_{MIT}) = \mu^o(N_{MIT})(1 - N_{MIT}/N)$. For the single-particle relaxation time one can show that multiple scattering effects give a small effect [17] and the lowest order results are nearly always a good approximation. This can be seen more explicitly in figure 10 of [17].

3. Numerical results for the mobility and for scattering times

3.1. Density dependent mass and mobility

In figure 1 we show the measured [15] effective mass m^* for electrons at the surface of (111) and our fit to these data by

$$m^*/m_e = \frac{0.47}{1 - N_{cm}/N} \tag{4}$$

with $N_{cm} = 2.2 \times 10^{11}$ cm^{-2} as the critical density of the divergent mass. m_e represents the free electron mass. The overall agreement is very good and we use this analytical formula in our expressions for the scattering times. Note, however, that even for $N \to \infty$ the effective mass is $m^* = 0.47m_e$, larger than the theoretical value $m^* = 0.36m_e$ [1].

In the following we discuss two models. One where the electron mass is kept constant $m^* = 0.36m_e$, independent of the electron density, and the other where the electron mass is density dependent according to equation (4). The disorder parameters for these two models, the

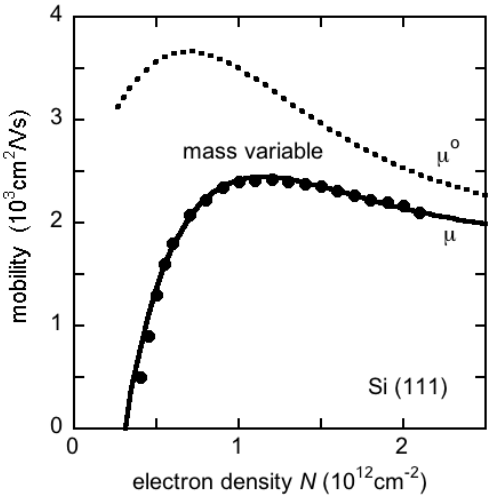

Figure 2. Mobility as a function of electron density N for silicon (111). The solid dots are experimental results of [15]. A density dependent electron mass was used in the calculation. The solid line (μ) represents our calculation where a metal–insulator transition is taken into account. The dotted line (μ^{o}) represents the lowest order calculation.

Table 1. Disorder parameters used for the model with 'mass constant', where $m^* = 0.36m_e$, and with 'mass variable', where $m^*/m_e = 0.46/(1 - N_{cm}/N)$ and $N_{cm} = 2.2 \times 10^{11}$ cm^{-2}.

	Disorder parameters			Density of MIT
Mass constant:	$N_i = 1.6 \times 10^{11}$ cm^{-2}	$\Delta = 3.6$ Å	$\Lambda = 56$ Å	$N_{MIT} = 3.5 \times 10^{11}$ cm^{-2}
Mass variable:	$N_i = 1.45 \times 10^{11}$ cm^{-2}	$\Delta = 3.2$ Å	$\Lambda = 57$ Å	$N_{MIT} = 3.1 \times 10^{11}$ cm^{-2}

impurity density N_i and the IRS parameters Δ and Λ are given in table 1. The electron density N_{MIT} of the MIT is also given in table 1.

In figure 2 we show the mobility versus density, together with experimental results [15]. The density dependent mass m^* is used in the calculation. Impurity scattering and interface-roughness scattering have been taken into account with an impurity density $N_i = 1.45 \times 10^{11}$ cm^{-2} at the Si/SiO$_2$ interface and IRS parameters $\Delta = 3.2$ Å and $\Lambda = 57$ Å, see table 1. The dotted line corresponds to a lowest order theory μ^{o} without an MIT. For the solid line μ an MIT at $N_{MIT} = 3.1 \times 10^{11}$ cm^{-2} was taken into account. We mention that $N_{MIT} > N_{cm}$ and we conclude that the mobility vanishes at N_{MIT} due to the MIT. Note that the mobility is directly related to a measured quantity, the conductivity $\sigma = Ne\mu$. In experiment one determines μ from σ. In our calculation we first determine the transport scattering time τ_t^{o} and then we calculate the mobility via $\mu = e\tau_t^{o}(1 - N_{MIT}/N)/m^*$. In fact, the mobility data of [15] have been used by fitting the theoretical mobility μ to the measured one in order to determine all parameters of disorder: N_i, Δ, Λ, and N_{MIT}.

The mobility data found in experiment [15] can also be fitted with a constant electron mass with equal accuracy, as in figure 2, for instance by using $m^* = 0.36m_e$, $N_i = 1.6 \times 10^{11}$ cm^{-2}, $\Delta = 3.6$ Å, $\Lambda = 56$ Å and $N_{MIT} = 3.5 \times 10^{11}$ cm^{-2}, see table 1. This is shown in figure 3 where a very good agreement is found between theory and experiment by taking into account an MIT. We conclude that by fitting mobility versus density data no valuable information can be obtained concerning a possible density dependence of the effective mass.

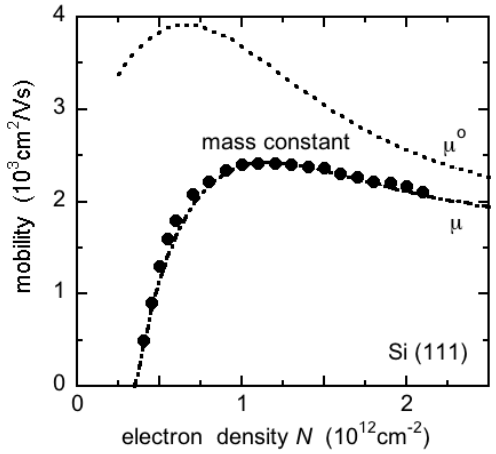

Figure 3. Mobility as a function of electron density N for silicon (111). The solid dots are the experimental results of [15]. A constant electron mass is used in the calculation. The dashed–dotted line (μ) represents our calculation where a metal–insulator transition is taken into account. The dotted line (μ^o) represents the lowest order calculation.

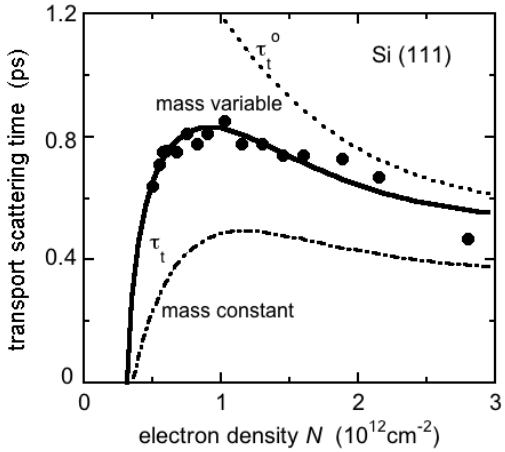

Figure 4. Transport scattering time as a function of electron density N for silicon (111). The solid dots are the experimental results of [15]. The solid and dotted lines represent our calculation with a density dependent electron mass. A metal–insulator transition is taken into account for the solid line. The lowest order result is represent by the dotted line. The dashed–dotted line represents a calculation with a constant electron mass, a metal–insulator transition is taken into account.

3.2. Transport scattering times and single-particle relaxation time

In figure 4 we compare the calculated transport scattering times τ_t and τ_t^o as a function of the electron density with experimental results [15]. For low density the experimental results for the transport scattering time show a tendency to decrease, in agreement with our theory, taking into account an MIT: we find $\tau_t \to 0$ at the MIT. The fact that we find agreement of the calculated mobility with the measured mobility in figure 2 also implies that the transport scattering times agree, when using the measured effective mass, which is density dependent. However, with a constant mass we would not find agreement between theory and experiment, see the dashed–dotted line in figure 4. We stress that the density dependent effective mass also

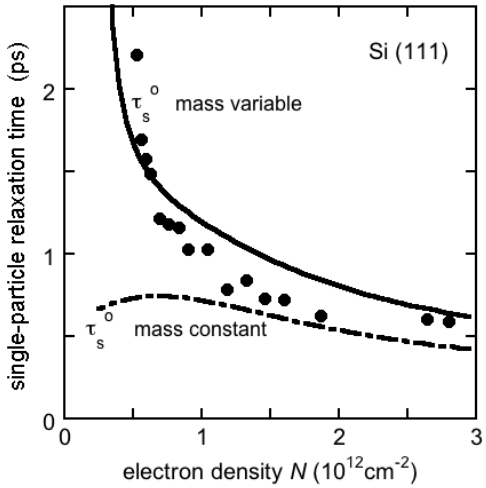

Figure 5. Single-particle relaxation time as a function of electron density N for silicon (111). The solid dots are experimental results of [15]. The solid line represents our calculation for a density dependent electron mass. The dashed–dotted line represents our calculation with a constant electron mass.

enters the calculation of the transport scattering time and is not only the connection between the mobility and the transport scattering time. For instance, the Fermi energy and the screening function depend on the effective mass. Without the introduction of multiple scattering effects and an MIT the scattering time τ_t^o shows a tendency to diverge at N_{cm}, see the dotted line in figure 4. This is in disagreement with experiment.

In figure 5 we show the calculated single-particle relaxation time τ_s^o versus electron density for a density dependent electron mass (solid line) and for a constant electron mass (dashed–dotted line). For the density dependent electron mass we obtained the astonishing result that τ_s^o increases with decreasing electron density and τ_s^o shows a tendency to diverge at the density where the effective mass diverges. This is in agreement with experimental results obtained from SdH measurements [15], see figure 5. For a constant electron mass τ_s^o does not show any sign of divergence near N_{cm}, see the dashed–dotted line in figure 5.

We mention that the single-particle relaxation time [15] is determined in an independent measurement, independent from the conductivity measurement, from which τ_t is determined. The fact that τ_s^o strongly increases near N_{cm} has its physical origin in the fact that the Bohr radius goes to zero when the mass diverges—screening becomes very efficient in this case. This is the reason for the strong enhancement of τ_s^o, the disorder becomes less important due to stronger screening.

From our numerical analysis we conclude that the agreement between theory and experiment for the transport properties of the 2DEG on the surface of silicon (111) is conditioned by two facts: that (i) an MIT occurs and that (ii) the effective mass shows a strong enhancement (divergence) at low electron density. For a constant electron mass one can explain the density dependence of the mobility, see figure 3, but the transport scattering time and the single-particle relaxation time from theory are no longer in agreement with the experimental results, see figures 4 and 5.

3.3. Metal–insulator transition

After decades of discussion there exists now some agreement that an MIT occurs in two-dimensional systems [8, 20, 22]. The origin of the mass divergence observed in silicon [5, 15]

is completely unclear. A recent theory [23], where a mass divergence due to many-body effects is found and where disorder is not taken into account, claims agreement with experiments concerning the critical density. However, the predictive power of this theory has not been worked out. The same holds for the theory of the MIT, as formulated in [22], where also a mass divergence is expected, however, in this case, induced by disorder. We mention that within the mode-coupling theory for the MIT due to multiple scattering [20] weak localization effects are neglected. This theory compares favorable with some experiments. In the mode-coupling theory the effective mass is an input parameter. In the present paper we have applied effective mass values obtained from experiment and we found good agreement between theory and experiment.

We have introduced the critical density of the MIT $N_{\mathrm{MIT}} \approx 3.1 \times 10^{11}$ cm^{-2} as a parameter determined from experiment. However, within the mode-coupling theory [20] one also can calculate the critical density for the MIT: the critical density is determined by the parameter A, which takes the value $A = 1$ at the transition point. The parameter A depends on the random potential, the screening function and the Lindhard function.

We used the values $N_{\mathrm{i}} = 1.45 \times 10^{11}$ cm^{-2}, $\Delta = 3.2$ Å, $\Lambda = 57$ Å, see table 1, and the density dependent effective mass according to equation (4) and found $N_{\mathrm{MIT}}^{\mathrm{cal}} = 3 \times 10^{11}$ cm^{-2}. This value is surprisingly near to the experimental value. But this very good agreement might be accidental. For a constant mass $m^* = 0.36 m_{\mathrm{e}}$ we used the values $N_{\mathrm{i}} = 1.6 \times 10^{11}$ cm^{-2}, $\Delta = 3.6$ Å, and $\Lambda = 56$ Å, see table 1, to calculate the critical density and found $N_{\mathrm{MIT}}^{\mathrm{cal}} = 2.0 \times 10^{11}$ cm^{-2}.

3.4. Comments concerning silicon (100)

For silicon (111) we used as critical parameters 2.2×10^{11} cm^{-2} $= N_{\mathrm{cm}} < N_{\mathrm{MIT}} = 3.1 \times 10^{11}$ cm^{-2}, which means that $N_{\mathrm{MIT}} = 1.4 N_{\mathrm{cm}}$. Therefore it is clear that for the transport scattering time and $N > N_{\mathrm{MIT}}$ multiple scattering effects are very important near $N \approx N_{\mathrm{MIT}}$ and at $N = N_{\mathrm{MIT}}$ the transport scattering time becomes zero.

In silicon (100) the transport scattering time shows at low density near $N > N_{\mathrm{cm}}$ a tendency to increase with decreasing density [24], similar to the single-particle relaxation time. According to our theory this means that in silicon (100) the relation $N_{\mathrm{MIT}} < N_{\mathrm{cm}}$ should hold and multiple scattering effects are not yet very important for $N > N_{\mathrm{cm}}$. A more detailed analysis of silicon (100) will be published elsewhere.

4. Discussion of the origin of the instability

4.1. Experimental results obtained with other material systems

In a recently studied high mobility GaAs heterostructure with peak mobility $\mu_{\mathrm{peak}} \approx 1 \times 10^7$ cm^2 V^{-1} s^{-1} and an MIT at $N_{\mathrm{MIT}} = 1.7 \times 10^9$ m^{-2} (this corresponds to $r_{\mathrm{s}} = 13.7$) a mass enhancement but no mass divergence was found for $r_{\mathrm{s}} < 13$ [11]. For thin AlAs quantum wells a sample with a peak mobility of $\mu_{\mathrm{peak}} \approx 5 \times 10^4$ cm^2 V^{-1} s^{-1} was studied in [10]. Only a mass enhancement of 2.2 at low density was found, and the 2DEG in AlAs showed an MIT at $N_{\mathrm{MIT}}^{\mathrm{AlAs}} \approx 0.7 \times 10^{11}$ cm^{-2}, without a mass divergence. In both systems, in GaAs heterostructures [11, 12] and in thin AlAs quantum wells [10], only one valley is available. This fact is our key argument to propose that the valley degeneracy $g_{\mathrm{v}} = 2$ is important for the mass divergence observed for electrons on the surface of silicon [6, 15]. We argue that in wide AlAs quantum wells, where $g_{\mathrm{v}} = 2$, the instability was not found in experiment [9] because of the reduced Coulomb interaction due to the large width $L > 12 a_{\mathrm{B}}^*$ of the quantum well. We

believe that this reduced Coulomb interaction leads to $N_{cm} \ll N_{MIT}$. We suggest that AlAs quantum wells with width $L \approx 5a_B^*$ and $g_v = 2$ should be used in order to search for the mass instability. Similar arguments hold for AlP.

4.2. Bloch's quantum phase transition

In [5] it was argued that a Stoner instability occurs at N_{cm}. However, later it was argued [6] that one has a 'spin-independent origin of the strongly enhanced effective mass'. This statement seems to be in contradiction to a Stoner instability. It was shown in [24] that the g-factor in silicon (100) is nearly independent of electron density and not critical at N_{cm}. This points to a non-ferromagnetic ground state for $N < N_{cm}$. Therefore, we suggest that in the electron gas on the surface of silicon (111) and (100) an instability occurs similar to the one proposed long ago by Bloch [25]. However, we argue that the symmetry broken ground-state at low electron density is presumably a valley-polarized state (or an antiferromagnetic state). In the original Bloch theory the new ground state at low density is a spin-polarized state with all spins oriented in the same direction, a ferromagnetic ground state. This is different to the ground state which we propose.

For the valley-polarized ground state the valley degeneracy factor at N_{cm} changes from $g_v = 2$ to 1. Such a transition was discussed some time ago [26, 27, 2]. The second possibility for the new ground state is an antiferromagnetic ground state where the spin degeneracy factor at N_{cm} changes from $g_s = 2$ to 1, however, we suppose there are antiparallel spin directions in the two valleys.

Within a one-valley electron gas, Monte Carlo calculations show that the transition to a ferromagnetic state occurs at $r_s \approx 25$ [28]. In experiment the mass divergence occurs near $r_s \approx 9.5$ [6, 15]. With $N \propto 1/r_s^2$ we conclude that for the critical electron density there is a factor 7.5 between Monte Carlo calculation and experiment. The valley-polarized ground state and the spin-polarized antiferromagnetic ground state were not found in Monte Carlo calculations because a model with only one valley was used, where such ground states are excluded from the very beginning.

The Bloch instability [25] has its origin in the fact that interaction effects favor a ferromagnetic (ordered) ground state, while the kinetic energy favors a paramagnetic (disordered) ground state. Near the MIT the screening properties of the electron gas change and for $N < N_{MIT}$ the screening effects of the electron gas are weakened, which means that Coulomb effects become stronger and more long-ranged in real space. This could be the reason why the Bloch instability happens near an MIT: the weaker screening properties of the localized states might help the ordered phase to become stable at higher electron density.

4.3. Spin or valley occupancy fluctuations

A *singular* mass behavior was observed in a three-dimensional heavy fermion system at the transition point from a paramagnetic to an antiferromagnetic ground-state [29]. For quantum phase transitions a diverging mass is expected at a quantum critical point [30]. The Bloch instability [25] is the first quantum phase transition discussed in the literature. This leads us to propose that for the electron gas on the surface of silicon (100) and silicon (111) the mass enhancement for electron densities near N_{cm} might be the *result* of the Bloch instability at N_{cm} due to fluctuations of the valley (or the spin) occupancy factor. For the valley (or spin) phase transition to occur at $N \approx N_{cm}$ electrons from one valley (spin direction) must be transferred to the other valley (spin direction). With the diverging mass at N_{cm} the Fermi energy of the electron gas vanishes. This allows the rapid redistribution of electrons from the two valleys

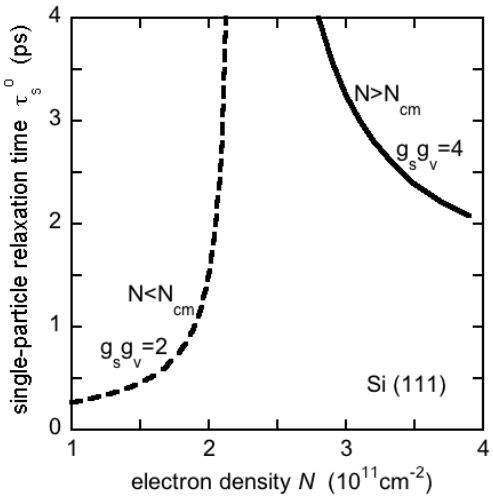

Figure 6. Single-particle relaxation time as a function of electron density N for silicon (111) for a density dependent electron mass. The solid line represents our calculation for a density dependent electron mass $m^*/m_e = 0.47/(1 - N_{cm}/N)$ with $N_{cm} = 2.2 \times 10^{11}$ cm^{-2} for $N > N_{cm}$ and $g_v g_s = 4$. The dashed line represents our calculation with $m^*/m_e = 0.47/(1 - N/N_{cm})$ for $N < N_{cm}$ and $g_v g_s = 2$.

(spin directions) into a single valley (spin direction) and vice versa. To say it differently, when the system becomes valley-polarized (spin-polarized) at low temperatures the Fermi energy increases by a factor two: $\varepsilon_F \to 2\varepsilon_F$. How can one populate, at temperatures $T \ll \varepsilon_F/k_B$, the energy ε states with $\varepsilon_F < \varepsilon < 2\varepsilon_F$ having only electrons with energy $0 < \varepsilon < \varepsilon_F$ available? With $m^* \to \infty$ we conclude that $\varepsilon_F \to 0$ and all states with $0 < \varepsilon < 2\varepsilon_F \to 0$ have the same energy and the redistribution can occur rapidly when valley fluctuations occur. Therefore, we suggest that the singular mass behavior near the instability point might be a general property of the Bloch instability and has its origin in quantum fluctuation effects.

4.4. Predictions and suggested experiments for $N < N_{cm}$

We expect that at low temperatures the effective mass is independent of temperature. The reason is that within the Bloch scenario above *and* below N_{cm} one has Fermi liquids with well-defined Fermi temperatures. This seems to be the case in experiment when $N > N_{cm}$ [15]. However, this will only be the case if temperatures are small compared to the effective Fermi temperature, defined with the density dependent effective mass. The effective Fermi temperature becomes very small near N_{cm}, where the effective mass becomes very large. We think that the prediction that $g_s g_v = 2$ for $N < N_{cm}$ can be tested in experiment: the Fermi energy should be a factor 2 larger than expected if the degeneracy factor were still $g_s g_v = 4$, as for $N > N_{cm}$. With SdH measurements one could get information about the degeneracy factor for $N < N_{cm}$.

We also propose to study samples where $N_{MIT} < N_{cm}$, for instance silicon (100) MOSFET structures, in the density range $N_{MIT} < N < N_{cm}$, where such samples should be metallic. By applying a parallel magnetic field one can spin-polarize the 2DEG and such experiments allow us to obtain information about the Fermi energy using magnetoresistance measurements [31].

It was suggested long ago that one should measure SdH oscillations in the insulating phase, where $N < N_{MIT}$, see figure 10 of [17]. In figure 6 we show the calculated single-particle relaxation time τ_s^o above and below N_{cm}, assuming a density dependent mass with a singularity

at the transition point. For $N > N_{cm}$ we use the effective mass as given in equation (4). For $N < N_{cm}$ we assume a diverging mass according to $m^*/m_e = 0.47/(1 - N/N_{cm})$ and we find that the single-particle relaxation time is not fully symmetric to $N = N_{cm}$. This is due to the weaker screening when the degeneracy is $g_s g_v = 2$. Figure 6 shows that the suggestion of the Bloch instability at $N = N_{cm}$ leads to a prediction for $N < N_{cm}$: a strongly increasing single-particle relaxation time is expected for N approaching N_{cm} from below.

5. Summary

We considered transport properties in a two-dimensional electron gas on the surface of silicon (111) with a divergent effective mass at N_{cm} and with a metal–insulator transition at $N_{MIT} = 1.4N_{cm}$. We find that near N_{MIT} the transport scattering time strongly decreases ($\tau_t \to 0$), while near N_{cm} the single-particle relaxation time strongly increases ($\tau_s^o \to \infty$). This behavior is in agreement with recent experiments [15]. The surprising behavior of τ_s^o near N_{cm} is the result of the mass divergence at N_{cm}: the screening effects increase with increasing effective mass.

As the origin for the mass divergence at the critical density N_{cm} we suggest a Bloch instability from a non-polarized paramagnetic ground state to a valley-polarized paramagnetic (or a spin-polarized antiferromagnetic) ground state with valley (or spin) occupancy fluctuations near N_{cm}. A Fermi liquid is expected for $N < N_{cm}$.

Acknowledgments

I thank L Fabie for putting the experimental data into the computer, which helped a lot to make good fits. I thank V T Dolgopolov and M Helm for stimulating discussions.

References

[1] Ando T, Fowler A B and Stern F 1982 *Rev. Mod. Phys.* **54** 437
[2] Gold A 1994 *Phys. Rev.* B **50** 4297
[3] Gold A 1985 *Phys. Rev. Lett.* **54** 1078
[4] Kravchenko S V, Kravcheno G V, Furneaux J E, Pudalov V M and D'Orio M 1994 *Phys. Rev.* B **50** 8039
[5] Shashkin A A, Kravchenko S V, Dolgopolov V T and Klapwijk T M 2001 *Phys. Rev. Lett.* **87** 086801
[6] Shashkin A A, Rahimi M, Anissimova S, Kravchenko S V, Dolgopolov V T and Klapwijk T M 2003 *Phys. Rev. Lett.* **91** 046403
[7] Shashkin A A, Anissimova S, Sakr M R, Kravchenko S V, Dolgopolov V T and Klapwijk T M 2006 *Phys. Rev. Lett.* **96** 036403
[8] Kravchenko S V and Sarachik M P 2004 *Rep. Prog. Phys.* **67** 1
Shashkin A A 2005 *Phys.—Usp.* **48** 129
[9] De Poortere E P, Tutuc E, Shkolnikov Y P, Vakili K and Shayegan M 2002 *Phys. Rev.* B **66** 161308
[10] Vakili K, Shkolnikov Y P, Tutuc E, De Poortere E P and Shayegan M 2004 *Phys. Rev. Lett.* **92** 226401
[11] Zhu J, Stormer H L, Pfeiffer L N, Baldwin K W and West K W 2003 *Phys. Rev. Lett.* **90** 056805
[12] Tan Y W, Zhu J, Stormer H L, Pfeiffer L N, Baldwin K W and West K W 2005 *Phys. Rev. Lett.* **94** 016405
[13] Estivals O, Kvon Z D, Gusev G M, Arnaud G and Portal J C 2004 *Physica* E **22** 446
[14] Gold A and Antonie O 2007 *Int. J. Mod. Phys.* B **21** 1529
[15] Shashkin A, Kapustin A A, Deviatov E V, Dolgopolov V T and Kvon Z D 2007 *Phys. Rev.* B **76** at press
(Shashkin A, Kapustin A A, Deviatov E V, Dolgopolov V T and Kvon Z D 2007 *Preprint* cond-mat0706.3552v1)
[16] Das Sarma S and Stern F 1985 *Phys. Rev.* B **32** 8442
[17] Gold A 1988 *Phys. Rev.* B **38** 10798

[18] Pines D and Nozieres P 1966 *The Theory of Quantum Liquids* vol 1 (New York: Benjamin)
[19] Jonson M 1976 *J. Phys. C: Solid State Phys.* **9** 3059
For a review see Singwi K S and Tosi M P 1981 *Solid State Phys.* **36** 177
[20] Gold A and Götze W 1986 *Phys. Rev.* B **33** 2495
Gold A 1989 *Appl. Phys. Lett.* **54** 2100
Gold A 1991 *Phys. Rev.* B **44** 8818
[21] Gold A 2000 *JETP Lett.* **72** 401
[22] Punnose A and Finkelstein A M 2005 *Science* **310** 289
[23] Khodel V A, Clark J W and Zverev M V 2005 *Europhys. Lett.* **72** 256
[24] Shashkin A A, Kravchenko S V, Dolgopolov V and Klapwijk T 2002 *Phys. Rev.* B **66** 073303
[25] Bloch F 1929 *Z. Phys.* **57** 545
[26] Bloss W J, Sham L J and Vinter B 1979 *Phys. Rev. Lett.* **43** 1529
[27] Ishihara A and Ioriatti L C Jr 1982 *Phys. Rev.* B **25** 5534
[28] Attaccalite C, Moroni S, Gori-Giorgi P and Bachelet G B 2002 *Phys. Rev. Lett.* **88** 256601
[29] v Löhneysen H, Pietrus T, Portich G, Schlager H G, Schröder A, Sieck M and Trappmann T 1994 *Phys. Rev. Lett.* **72** 3262
[30] Coleman P and Schofield A J 2005 *Nature* **433** 226
[31] Dolgopolov V T and Gold A 2000 *JETP Lett.* **71** 27
Gold A and Dolgopolov V T 2003 *Physica E* **17** 280